Published OnlineFirst February 16, 2010; DOI: 10.1158/1078-0432.CCR-09-1873

Human Cancer Biology

Clinical Cancer Research

Critical Role of $G\alpha_{12}$ and $G\alpha_{13}$ for Human Small Cell Lung Cancer Cell Proliferation *In vitro* and Tumor Growth *In vivo*

Marius Grzelinski[1], Olaf Pinkenburg[1], Thomas Büch[2], Maike Gold[1], Stefanie Stohr[2], Hermann Kalwa[1], Thomas Gudermann[2], and Achim Aigner[1]

Abstract

Purpose: In small cell lung cancer cells (SCLC), various autocrine stimuli lead to the parallel activation of $G_{q/11}$ and $G_{12/13}$ proteins. Although the contribution of the $G_{q/11}$-phospholipase C-β cascade to mitogenic effects in SCLC cells is well established, the relevance of $G_{12/13}$ signaling is still elusive. In other tumor entities, $G_{12/13}$ activation promotes invasiveness without affecting cellular proliferation. Here, we investigate the role of $G_{12/13}$-dependent signaling in SCLC.

Experimental Design: We used small hairpin RNA–mediated targeting of $G\alpha_{12}$, $G\alpha_{13}$, or both in H69 and H209 cells and analyzed the effects of $G\alpha_{12}$ and/or $G\alpha_{13}$ knockdown on tumor cells *in vitro*, tumor growth *in vivo*, and mitogen-activated protein kinase (MAPK) activation.

Results: Lentiviral expression of small hairpin RNAs resulted in robust and specific $G\alpha_{12}$ and $G\alpha_{13}$ knockdown as well as markedly inhibited proliferation, colony formation, and bradykinin-promoted stimulation of cell growth. Analyzing the activation status of all three major MAPK families revealed nonredundant functions of $G\alpha_{12}$ and $G\alpha_{13}$ in SCLC and a marked p42/p44 activation upon $G\alpha_{12}/G\alpha_{13}$ knockdown. In a s.c. tumor xenograft mouse model, $G\alpha_{12}$ or $G\alpha_{13}$ downregulation led to decreased tumor growth due to reduced tumor cell proliferation. More importantly, $G\alpha_{12}/G\alpha_{13}$ double knockdown completely abolished H69 tumorigenicity in mice.

Conclusions: $G\alpha_{12}$ and $G\alpha_{13}$ exert a complex pattern of nonredundant effects in SCLC, and in contrast to other tumor types, SCLC cell proliferation *in vitro* and tumorigenicity *in vivo* critically depend on $G_{12/13}$ signaling. Due to the complete abolishment of tumorgenicity in our study, RNAi-mediated double knockdown may provide a promising new avenue in SCLC treatment. *Clin Cancer Res; 16(5); 1402–15. ©2010 AACR.*

Members of the G protein–coupled receptor (GPCR) superfamily are involved in the regulation of virtually all cellular processes, and G protein–dependent signaling pathways have been shown to play a pivotal role in the pathogenesis of tumors. Heterotrimeric G proteins are composed of a guanine nucleotide binding α-subunit and a βγ dimer. Based on sequence homologies, four families of G protein-α subunits can be distinguished, i.e., G_S, $G_{i/o}$, $G_{q/11}$, and $G_{12/13}$ (1–3). The constitutive activation of GPCRs or G proteins has been shown in various tumor entities and is implicated in cellular proliferation, regulation of apoptosis, enhanced cell motility and invasiveness, metastatic potential of tumor cells, as well as angiogenic effects (4, 5). Although the diversity of G protein–dependent functions in tumor cells is mirrored by the fact that G proteins of all four families have been identified as potential oncogenes, the $G_{12/13}$ family has attracted particular interest in cancer research because its members have been described to promote the growth and oncogenic transformation of murine fibroblasts (6, 7) and $G_{12/13}$ proteins have been invoked in tumorigenesis (8). $G\alpha_{12}$ was first described as *gep* oncogene in soft tissue sarcomas. The expression of wild-type (WT) $G\alpha_{12}$ in fibroblasts turned out to be sufficient for cell transformation (6). More recently, a role of $G_{12/13}$ signaling has been shown in breast and prostate cancer (9, 10). In these tumors, $G_{12/13}$-dependent signaling was shown to regulate tissue invasiveness and metastatic capacity, but not proliferation of tumor cells. This observation is in line with the well-characterized ability of $G_{12/13}$ to activate monomeric GTPases of the Rho family and, thus, to control cytoskeletal proteins and cellular motility (11).

Authors' Affiliations: [1]Department of Pharmacology and Toxicology, Philipps-University School of Medicine, Marburg, Germany and [2]Walther-Straub-Institute for Pharmacology and Toxicology, University of Munich, Germany

Note: Supplementary data for this article are available at Clinical Cancer Research Online (http://clincancerres.aacrjournals.org/).

M. Grzelinski, O. Pinkenburg, and T. Büch contributed equally to the work.

Corresponding Authors: Achim Aigner, Department of Pharmacology and Toxicology, Philipps-University Marburg, Karl-v.-Frisch-Strasse 1, D-35033 Marburg, Germany. Phone: 49-6421-286-2262; Fax: 49-6421-286-5600; E-mail: aigner@staff.uni-marburg.de or Thomas Gudermann, Walther-Straub-Institute of Pharmacology and Toxicology, University of Munich, Goethestr. 33, D-80336 Munich, Germany. Phone: 49-89-2180-75700; Fax: 40-89-2180-75701; E-mail: Thomas.Gudermann@lrz.uni-muenchen.de.

doi: 10.1158/1078-0432.CCR-09-1873

Published OnlineFirst February 16, 2010; DOI: 10.1158/1078-0432.CCR-09-1873

Translational Relevance

Small cell lung cancer (SCLC) displays the most aggressive clinical course among all common types of pulmonary tumors, and the poor survival rates emphasize the need for novel treatment strategies based on a deeper understanding of the molecular events underlying SCLC tumorigenesis and tumor progression. Various autocrine stimuli lead to the parallel activation of $G_{q/11}$ and $G_{12/13}$ proteins; however, the relevance of $G_{12/13}$ signaling is still elusive. In this study based on small hairpin RNA (shRNA)–mediated knockdown of $G\alpha_{12}$ and/or $G\alpha_{13}$, we investigate the role of $G_{12/13}$-dependent signaling on SCLC tumor cells *in vitro*, tumor growth *in vivo*, and mitogen-activated protein kinase activation. We show that $G\alpha_{12}$ and $G\alpha_{13}$ exert a complex pattern of nonredundant effects in SCLC and show that, in contrast to other tumor types, SCLC cell proliferation *in vitro* and tumorigenicity *in vivo* critically depend on $G_{12/13}$ signaling. Strikingly, $G\alpha_{12}/G\alpha_{13}$ double knockdown completely abolishes H69 tumorigenicity in mice. Although the inhibition of single G protein–coupled receptors or G protein–coupled receptor agonists may be insufficient for treatment, we show that the parallel knockdown of $G\alpha_{12}$ and $G\alpha_{13}$ as point of convergence may provide a promising new avenue in SCLC treatment.

Lung cancer accounts for over 200,000 new cases and over 160,000 deaths per year in the United States. Small cell lung cancer (SCLC) displays the most aggressive clinical course among all types of pulmonary tumors. Although current chemotherapy regimen clearly show clinical benefit, the overall survival after 5 years is still only 7% to 12% (12), and patients with SCLC tend to develop distant metastases. This situation clearly emphasizes the need for novel treatment strategies based on a deeper understanding of the molecular events underlying SCLC tumorigenesis and tumor progression.

SCLC cells have been shown to secrete a plethora of GPCR ligands, e.g., acetyl choline or neuropeptides such as bradykinin, bombesin/gastrin-releasing peptide, or galanin, which act as principal mitogenic stimuli (13, 14). Owing to the critical role of G protein signaling for the control of proliferation in SCLC cells, many efforts have been made to use blockers of mitogenic GPCRs expressed in SCLC as therapeutic tools (15–19). However, the redundance of multiple autocrine loops in SCLCs promoting the activation of numerous distinct GPCRs limits the therapeutic efficacy of this approach. Thus, points of convergence of mitogenic GPCR signaling in SCLC cells could turn out as more promising therapeutic targets. The GPCRs that regulate proliferation in SCLC cells couple to $G_{q/11}$ and $G_{12/13}$ proteins, leading to the parallel activation of the $G_{q/11}$-phospholipase C-Ras-extracellular signal-regulated kinase (ERK) 1/2 and the $G_{12/13}$-Rho signaling pathways (20). Although activation of $G_{q/11}$ and phospholipase Cβ causes an increase in intracellular calcium ($[Ca^{2+}]_i$), which is necessary and sufficient to activate the Ras-Raf-ERK1/2 cascade in SCLC cells (21), $G_{12/13}$ signaling in SCLC cells has been implicated in the regulation of cell motility and metastasis (22, 23) and in the induction of proapoptotic pathways through the activation of c-Jun-NH_2-kinase (24). However, the relative contribution of $G_{q/11}$ and $G_{12/13}$-dependent signaling cascades to the cellular phenotype of SCLC cells is presently unknown (21). Furthermore, previous studies suggest different biological effects of G_{12} and G_{13} (25), thus emphasizing the need to assess the functional relevance of both G proteins separately.

In this article, we aimed at the selective disruption of G_{12} and G_{13} function to decipher the role of these proteins for oncogenic signaling in SCLC cells. To this end, we used RNAi-mediated downregulation of the α-subunits of G_{12} and G_{13} ($G\alpha_{12}$ and $G\alpha_{13}$), alone or in combination, by infection of H69 and H209 SCLC cells with shRNA constructs using a lentiviral system. Single targeting revealed profound antiproliferative effects in response to $G\alpha_{12}$ or $G\alpha_{13}$ downregulation. The analysis of the activation status of all three major mitogen-activated protein kinase (MAPK) families revealed nonredundant functions of $G\alpha_{12}$ and $G\alpha_{13}$ in SCLC as well as a marked p42/p44 activation upon $G\alpha_{12}/G\alpha_{13}$ knockdown. In a s.c. tumor xenograft mouse model, $G\alpha_{12}$ or $G\alpha_{13}$ single knockdown led to a markedly reduced tumor growth based on decreased tumor cell proliferation. More importantly, $G\alpha_{12}/G\alpha_{13}$ double targeting resulted in complete abolishment of tumor growth. Thus, we show for the first time that both $G\alpha_{12}$ and $G\alpha_{13}$ play a critical and nonredundant role in SCLC proliferation *in vitro* and *in vivo*, and that selectively interfering with G_{12} and G_{13} signaling, e.g., through RNAi-mediated therapeutic blockage of both G proteins, may provide a promising new avenue in SCLC treatment.

Materials and Methods

Cell lines, viral shRNA constructs, and stable transfection. Lung cancer cell lines were obtained from the American Type Culture Collection and were cultivated under standard conditions (37°C, 5% CO_2) in RPMI (PAA) supplemented with 10% FCS unless indicated otherwise. Oligonucleotides for the generation of shRNA were designed according to established rules (26, 27), and the DNA sequences detailed in Supplementary Table S1 were chemically synthesized (MWG Biotech). Using the BglII and HindIII restriction sites, the oligonucleotides were cloned into the pSUPER vector and correct insertion was controlled by sequencing. Subsequently, the H1-cassettes of the pSUPER vectors were cloned into the lentivirus vector pLVTHM using ClaI and BamHI. To generate recombinant viruses, 20 μg/10-cm dish of the *cis*-vector pLV-12-1, pLV-12-2, pLV-12-3 ($G\alpha_{12}$-specific shRNAs), pLV-13-1, pLV-13-2, pLV-13-3 ($G\alpha_{13}$-specific shRNAs), pLV-UR-1,

Published OnlineFirst February 16, 2010; DOI: 10.1158/1078-0432.CCR-09-1873

pLV-UR-2, or pLV-UR-3 (control shRNAs) were cotransfected into HEK cells together with 15 μg psPAX2 ("trans plasmid") and with 6 μg pMD2G (VSV-G) using the calcium phosphate precipitation method. Six to 8 h after transfection, the medium was changed, and 2 d later, the supernatant was collected and sterile filtered. Viruses were purified and concentrated using sucrose sedimentation (20% sucrose in TBS, 26,000 rpm, 2 h) and were resuspended in complete RPMI. The viral titer was determined by serial dilution in HEK cells. H69 and H209 cells were transduced with 20 transducing units of recombinant virus.

RNA preparation and quantitative reverse transcription-PCR. Total RNA from tumor cells or homogenized tissues was isolated using the Tri reagent (PEQLAB) according to the manufacturer's protocol. For tissue homogenization, tissues were mixed with 1 mL Tri reagent and homogenized before RNA preparation. Reverse transcription was done using the RevertAid H Minus First Strand cDNA Synthesis kit from Fermentas as follows: 2 μg total RNA and 1 μL random hexamer primer (0.2 μg/μL) were diluted in DEPC-treated water to a final volume of 11 μL, incubated at 70°C for 5 min and chilled on ice before adding 4 μL 5× reaction buffer, 0.5 μL RNase inhibitor (20 u/μL), 2 μL 10 mmol/L deoxynucleotide triphosphate mix, and 1.5 μL DEPC-treated water. After incubation at 25°C for 5 min, 1 μL reverse transcriptase (200 u/μL) was added, and the mixture was incubated for 10 min under the same conditions and for 60 min at 42°C, before stopping the reaction by heating at 70°C for 10 min and chilling on ice. Quantitative PCR was done in a LightCycler from Roche using the Absolute QPCR SYBRGREEN Capillary Mix (Abgene) according to the manufacturer's protocol with 4 μL cDNA (diluted 1:100), 1 μL primers (5 μmol/L each), and 5 μL SYBR Green master mix. A preincubation for 15 min at 95°C was followed by 55 amplification cycles: 10 s at 95°C, 10 s at 55°C, and 10 s at 72°C. The melting curve for PCR product analysis was determined by rapid cooling down from 95°C to 65°C, and incubation at 65°C for 15 s before heating to 95°C. To normalize for equal mRNA/cDNA amounts, PCRs with $G\alpha_{12}$- or $G\alpha_{13}$-specific and with actin-specific primer sets were always run in parallel for each sample, and $G\alpha_{12}/G\alpha_{13}$ levels were determined by the formula 2^{CP}(G protein) /2^{CP}(actin) in which *CP* is the cycle number at the crossing point (0.3).

Growth assays. For proliferation studies, cell lines were plated into 96-well plates at 2,000 to 4,000 cells per well and 5 wells per time point, and cultivated in RPMI/10% FCS in a humidified incubator under standard conditions. The numbers of viable cells were assessed using a colorimetric assay according to the manufacturer's protocol (Cell Proliferation Reagent WST-1, Roche Molecular Biochemicals), or were counted microscopically using a Neubauer chamber. Where indicated, 1 μmol/L ERK 1/2 inhibitor U0126 (Promega) or 10 μmol/L Rho kinase inhibitor Y27632 (Sigma, dissolved in DMSO) was added with appropriate volumes of DMSO serving as negative controls. The role of Rho in cellular proliferation was also addressed by using a clostridial C3 fusion protein together with the activated C2II binding component of C. botulinum C2 toxin (both were kindly provided by Holger Barth, Ulm, Germany). For this purpose, the cells were treated with the fusion toxin at 200 ng/mL, a concentration reliably inactivating Rho proteins (see e.g., ref. 28). For bradykinin stimulation experiments, a 10-mmol/L bradykinin stock solution, prepared in 5% acetic acid, was diluted in PBS and added to the wells containing RPMI/10% FCS to a final concentration of 100 nmol/L, with the appropriate negative controls.

To study proliferation of the cell lines in a gel matrix, soft agar assays were carried out essentially as described in ref. (29). Briefly, 100,000 cells in 0.35% agar (Bacto Agar, Becton Dickinson) were layered on top of 1 mL of a solidified 0.6% agar layer in a 35-mm dish. Growth media with 10% FCS were included in both layers. Colonies of >50 μm in diameter were counted after 2 to 3 wk of incubation by an image analyzer or by at least two independent blinded investigators.

Tumor growth in nude mice. WT or stably infected H69 cells (3×10^6) in 150 μL PBS were injected s.c. into both flanks of athymic nude mice (*nu/nu*) with 10 tumors per cell line. When solid tumors became visible after 1 wk, tumor growth was monitored every 2 to 3 d as indicated in the figure, and tumor sizes were determined from the product of the perpendicular diameters of the tumors. After 4 wk, mice were sacrificed and tumors were removed. Three pieces of each tumor representing approximately half of the tumor mass were immediately fixed in 10% paraformaldehyde for paraffin embedding and the other half was shock frozen in liquid nitrogen for RNA extraction. In the case of H209 cell lines, 5×10^6 cells were injected, and after 4 wk, mice with well-established tumors below 100 mm^3 were selected for the subsequent monitoring of tumor growth rates as described above.

Immunohistochemistry. Paraffin sections of each tumor contained different pieces of the tumor mass. Immunostaining was done essentially as previously described (30). Briefly, after deparaffinization with xylene and rehydration with graded alcohols, sections were incubated in 10 mmol/L citrate buffer (pH 7.4) at 90°C for 20 min, endogenous peroxidases were inactivated with 0.3% hydrogen peroxide at 4°C for 20 min, and slides were washed thrice with PBS/0.1% Tween 20. After blocking with 10% normal goat serum or normal horse serum in PBS/0.1% Tween 20/2% bovine serum albumin for 1 h at room temperature, the slides were incubated with the antibodies anti-G12 (Santa Cruz, 1:200), anti-G13 (Santa Cruz, 1:200), or anti–proliferating cell nuclear antigen (PCNA; DAKO, 1:200) in PBS/0.1% Tween 20 at 4°C overnight in a wet chamber. After washing, a 1:500 diluted, biotinylated goat anti–(rabbit-IgG) or horse anti–(mouse-IgG) antibody (Vector Laboratories; 1:500) was applied as the secondary antibody for 1 h before washing. Immunoreactivity on the sections was visualized using a streptavidin-biotin-peroxidase complex (ABC kit, Vector Laboratories) according to the manufacturer's instructions, with diaminobenzidine as peroxidase substrate (brown). PCNA-stained

Published OnlineFirst February 16, 2010; DOI: 10.1158/1078-0432.CCR-09-1873

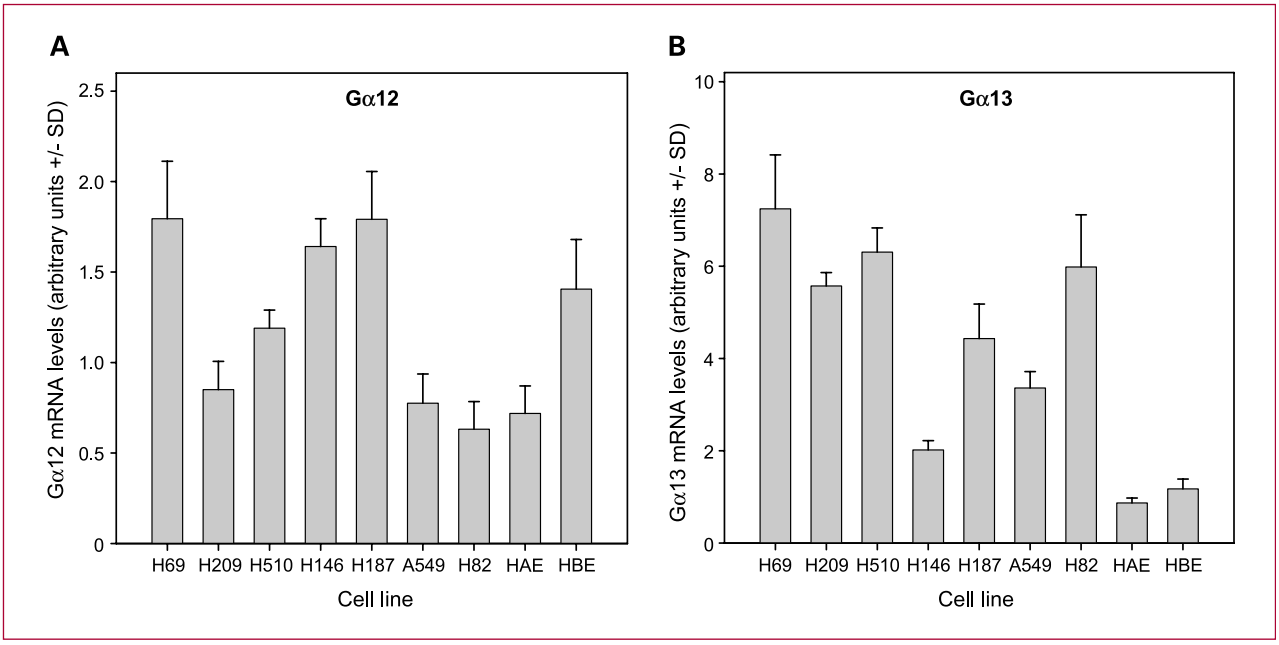

Fig. 1. Expression levels of Gα12 (A) and Gα13 (B) in various SCLC and NSCLC cell lines, as determined by quantitative RT-PCR. Values are normalized for actin as described in Materials and Methods and presented in arbitrary units.

sections were counterstained with hematoxylin, mounted, and analyzed light microscopically by three blinded observers. For the quantitation of G12 and G13 levels, the counterstain was omitted, and upon mounting, slides were light microscopically scanned and electronically analyzed for intensities of brown staining (TILL Photonics and TILL Vision).

Antibody arrays. To analyze the phosphorylation status of various MAPKs in control versus $G\alpha_{12}$ or control versus $G\alpha_{13}$ knockdown cells, proteome profiler antibody arrays (R&D) were used according to the manufacturer's instructions. Briefly, after preincubation in Array buffer 1, arrays were incubated overnight at 4°C in 250 μL or the respective cell lysate in Lysis buffer 6/1,250 μL Array buffer 1. After washing, arrays were incubated in a 1:100 dilution of the Detection Antibody Cocktail Concentrate for 2 h at room temperature and washed again. Bound antibodies were detected using Streptavidin-horseradish peroxidase (1:2,000, 30 min at room temperature), and after another washing step, signals were visualized by incubation of the arrays in the LumiGLO chemiluminescent reagent and parallel film exposure (Hyperfilm, Amersham). To accurately determine signals of different intensities, films were exposed between 5 s and 10 min, and signals above the background and below the film saturation were scanned and quantitated using the ImageJ software.

Western blots. For Western blot analysis, SCLC cells were grown in six-well plates coated with poly-L-lysine (6×10^5 cells per well) for 24 h. Cells were washed with ice-cold PBS and lysed in 200 μL of lysis buffer [125 mmol/L Tris-HCl, 2% (w/v) SDS, 10% (v/v) glycerol, 50 μg/mL bromphenol blue]. Proteins were separated by SDS-PAGE (9% gel) and electroblotted onto Hybond C Extra membranes. Membranes were incubated in Rotiblock (Roth) for 1 h to saturate nonspecific binding sites, washed in PBS, and incubated with the respective primary antibody at 4°C overnight. Phosphorylated p44/42 MAPK was detected using a phospho-specific anti-p44/42 MAPK mouse monoclonal antibody (Santa Cruz Biotechnology, 1:500). Phosphorylated MYPT1 (Threonine 853) was detected using a phospho-specific monoclonal antibody from a rabbit (New England Biolabs, 1:1,000). Antibodies against the Gα subunits of G_{12} and G_{13} were from Santa Cruz (1:500). Reprobing for loading controls was done using an anti-p44/42 MAPK mouse monoclonal antibody detecting total (phosphorylated and unphosphorylated) ERK. Western blots were developed by chemiluminescence as described above.

Data analysis. For statistical analysis, Student's unpaired, two-sided *t* test was used for comparisons between data sets. Unless indicated otherwise, bars represent the means of at least three independent experiments. For cost reasons, the antibody array was done only once, and representative results were subsequently confirmed by Western blotting in independent experiments with fresh cell lysates. The immunohistochemical analysis was done in all tumor xenografts ($n = 10$) with at least three fields per section being randomly selected for microscopic quantitation. Error bars in the figures represent SDs.

Results

Determination of Gα12 and Gα13 expression levels in lung cancer cell lines. $G\alpha_{12}$ and/or $G\alpha_{13}$ expression levels were determined by quantitative reverse transcription-PCR (RT-PCR) in the classic SCLC lines H69, H209, H510, H146,

Published OnlineFirst February 16, 2010; DOI: 10.1158/1078-0432.CCR-09-1873

and H187. Additionally, the non-SCLC lines A549, HAE, and HBE as well as the nonclassic SCLC line H82 were included. All cell lines were positive for $G\alpha_{12}$ (Fig. 1A) and $G\alpha_{13}$ (Fig. 1B), with approximately 2- to 2.5-fold differences in $G\alpha_{12}$ expression levels independent of the origin of the cell lines (SCLC or non-SCLC). $G\alpha_{13}$ expression showed larger variations with ~15-fold differences between the highest and the lowest $G\alpha_{13}$-expressing cell line. Notably, no correlation was found between $G\alpha_{12}$ and $G\alpha_{13}$ expression levels. For subsequent experiments, we selected the SCLC cell lines H69, which showed the highest expression levels of both $G\alpha_{12}$ and $G\alpha_{13}$, and H209 with lower $G\alpha_{12}$ and high $G\alpha_{13}$ expression.

RNAi-mediated depletion of Gα12 and Gα13 in SCLC cells. Initial experiments revealed that nonviral transfection efficacies in H69 and H209 cells were extremely poor. Despite the fact that the use of a recently described low-molecular weight polyethylenimine (31) resulted in somewhat higher efficacies in DNA uptake and expression compared with several other transfection agents, we chose a viral approach for expressing shRNA constructs to induce RNAi-mediated $G\alpha_{12}$ and/or $G\alpha_{13}$ knockdown. shRNA expression plasmids were constructed by cloning the DNA oligonucleotides detailed in Supplementary Table S1 into an enhanced green fluorescent protein (EGFP) expression vector. Upon viral infection with these constructs, transcription is expected to result in a partially double-stranded RNA sequence (boxed in Supplementary Table S1) being recognized by Dicer and thus qualifying for the specific induction of RNA interference according to the rules of

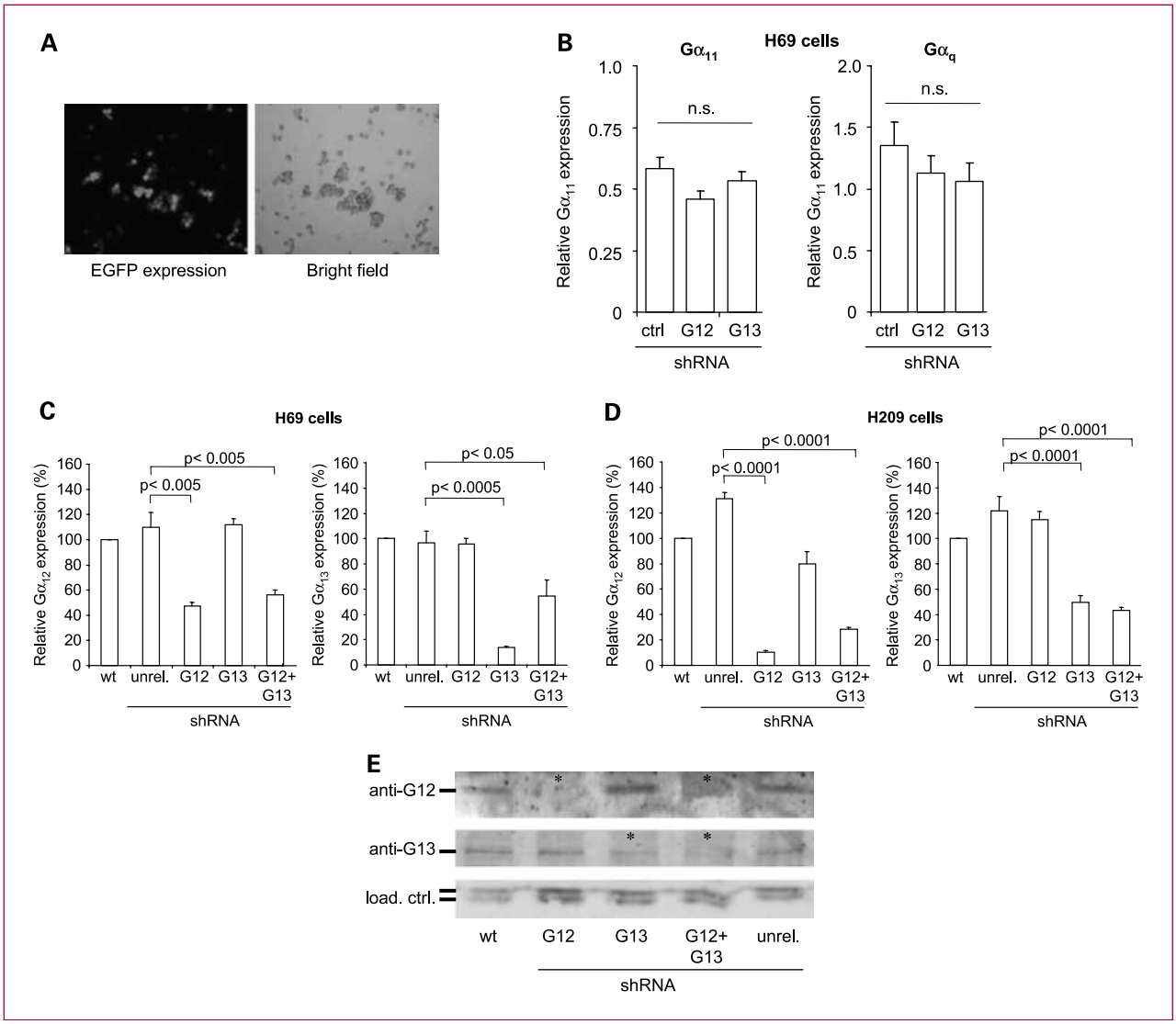

Fig. 2. A, viral infection of SCLC cells with shRNA constructs, as determined by EGFP expression in fluorescence microscopy (left). The comparison with bright-field microscopy (right) reveals an ~100% efficacy. B, upon $G\alpha_{12}$ or $G\alpha_{13}$ knockdown in H69 cells, levels of $G\alpha_{11}$ and $G\alpha_q$ remain unchanged. C and D, specific targeting efficacies of $G\alpha_{12}$ shRNA (left) and $G\alpha_{13}$ shRNA (right) in H69 (C) and H209 (D) cells (WT, 100%). E, Western blots for $G\alpha_{12}$ and $G\alpha_{13}$ in H69 cells reveal the specific knockdown of $G\alpha_{12}$ and $G\alpha_{13}$ protein levels (*).

Published OnlineFirst February 16, 2010; DOI: 10.1158/1078-0432.CCR-09-1873

Table 1. Tumor takes upon injection of the infected cells, i.e., percentage of visible tumors of 10 s.c. injections per group, reveal a complete loss of tumorigenicity upon $G\alpha_{12}/G\alpha_{13}$ double targeting

shRNA	Percentage of visible tumors
WT	70
G12	20
G13	70
G12 + 13	0
Unrelated	90

Reynolds et al. and Elbashir et al. (26, 27). Cellular EGFP expression upon viral infection allowed the simultaneous assessment of DNA uptake efficacy. The morphologic analysis of the cells by fluorescence microscopy revealed an infection efficiency of ~100% (Fig. 2A).

H69 cells virally infected with shRNA constructs were analyzed by quantitative RT-PCR to evaluate the depletion of $G\alpha_{12}$ and/or $G\alpha_{13}$. To avoid nonspecific small interfering RNA effects, which have been previously described and may obscure any gene-specific biological effects (see, e.g., ref. 35 for review), three different constructs per target gene and three control shRNAs (Supplementary Table S1) were used and tested independently for targeting efficacy and antiproliferative effects. Quantitative RT-PCR revealed that $G\alpha_{12}$-targeting shRNAs 12-1 and 12-2 were similarly efficient, as well as all three $G\alpha_{13}$-targeting shRNAs. Proliferation assays showed a concomitant reduction in cell proliferation (see below). Based on the targeting efficacies and antiproliferating effects, constructs 12-1 and 13-1 were selected for subsequent experiments.

The $G\alpha_{12}$-targeting shRNA downregulated $G\alpha_{12}$ mRNA in H69 and H209 cells by >50% and ~90%, respectively, when compared with control-infected or WT (i.e., parental, nontransduced) cells (Fig. 2C and D, left). $G\alpha_{13}$ levels remained unchanged, proving the specificity of gene targeting. Likewise, $G\alpha_{13}$-specific shRNAs resulted in a profound 50% to 85% reduction of $G\alpha_{13}$ mRNA levels in both cell lines, without affecting $G\alpha_{12}$ (Fig. 2C and D, right). Gene-specific and similar targeting efficacies were also observed upon double infection with both shRNA constructs (Fig. 2C and D). Likewise, specific knockdown was observed on the protein level. Western blots revealed the absence or near absence of $G\alpha_{12}$ or $G\alpha_{13}$ bands, respectively, upon single and double knockdown (Fig. 2E, *). Because these bands were below the limit of detection, no quantitation was possible. In contrast, mRNA levels of other G proteins, Gα11 and Gαq, remained unchanged upon $G\alpha_{12}$ or $G\alpha_{13}$ knockdown (Fig. 2B). The fact that highly reproducible data were obtained when using the various $G\alpha_{12}$- or $G\alpha_{13}$-specific versus unrelated shRNA constructs confirmed the suitability of our approach for the specific depletion of $G\alpha_{12}$ and $G\alpha_{13}$, and the correlation between knockdown efficiencies and antiproliferative effects suggests the absence of nonspecific off-target effects.

$G\alpha_{12}/G\alpha_{13}$ dependence of SCLC cell proliferation. Monitoring the cell proliferation of H69 cells infected with $G\alpha_{12}$ and/or $G\alpha_{13}$-shRNA constructs over several days revealed a markedly reduced proliferative capacity upon $G\alpha_{12}$ or $G\alpha_{13}$ depletion. More specifically, $G\alpha_{13}$ targeting led to a ~50% reduction in cell number, whereas upon $G\alpha_{12}$ depletion, a more profound inhibitory effect (>60%) on cell proliferation was observed compared with WT or control-infected cells (Fig. 3A). This effect was observed for all constructs that showed gene targeting efficacy, i.e., shRNAs 12-1, 12-2, 13-1, 13-2, and 13-3, but not for shRNA 12-3 with no targeting and no antiproliferative activities, thus confirming the specificity of the active shRNAs and suggesting the absence of nonspecific effects. Furthermore, the proliferation data showed identical results of WT cells and those infected with unrelated control shRNA, thereby excluding nonspecific effects intrinsically due to viral infection (Fig. 3A). Double targeting, i.e., the combined infection with both constructs, resulted in antiproliferative effects similar to the results after single targeting (Fig. 3A). Thus, the knockdown of both $G\alpha_{12}$ and $G\alpha_{13}$ did not produce a synergistic growth-inhibiting effect *in vitro*. Next, we performed soft agar assays that more closely resemble the *in vivo* situation. In H69 cells, colony formation was markedly reduced by approximately 50% to 65% upon $G\alpha_{12}$ or $G\alpha_{13}$ targeting. Combined infection with shRNA constructs targeting both gene products yielded similar results (Fig. 3B). These results were confirmed in the second SCLC cell line investigated, H209 cells. While due to poor colony formation, soft agar assays could not be done, WST-1-based proliferation assays revealed proliferation rates that were profoundly reduced by approximately 50% to 65% upon viral $G\alpha_{12}$ or $G\alpha_{13}$ shRNA infection (Fig. 3C). Double targeting of both $G\alpha_{12}$ and $G\alpha_{13}$ led to comparable results, again reflecting the lack of an additive antiproliferative effect upon the knockdown of both proteins (Fig. 3C).

G_{12}/G_{13} proteins have previously been shown to signal through Rho kinases. Thus, decreased Rho kinase activity may entail antiproliferative effects. To test this possibility, H69 and H209 WT cells were treated with the Rho kinase inhibitor Y27632 (10 μmol/L) and cell proliferation was compared with nontreated WT cells. As shown in Fig. 3A and B, no differences were observed in H69 and H209 cells, indicating that Rho kinase activation does not play a major role for the antiproliferative effects emanating from $G\alpha_{12}$ and/or $G\alpha_{13}$ targeting. To confirm the efficacy of the Rho kinase inhibitor Y27632 in our cells, we determined the phosphorylation of MYPT1, which is the regulatory unit of myosine phosphatase. Upon activation of Rho, MYPT1 is phosphorylated by Rho kinase at Threonine 696, leading to an inhibition of the myosine phosphatase holoenzyme (see ref. 32 for review). Consequently, treatment of H69 WT cells with Y27632 (10 μmol/L,

Published OnlineFirst February 16, 2010; DOI: 10.1158/1078-0432.CCR-09-1873

1 hour) completely abolished basal MYPT1 phosphorylation (Supplementary Fig. S1, lanes 1 and 2). Interestingly, a similarly pronounced reduction of MYPT1 phosphorylation in H69 cells independent of the presence or absence of inhibitor was observed upon the shRNA-mediated downregulation of $G\alpha_{12}/G\alpha_{13}$ (Supplementary Fig. S1, lanes 3 and 4 versus lane 1), most probably reflecting the impaired Rho/Rho kinase signaling following $G\alpha_{12}/G\alpha_{13}$ knockdown.

In line with the observed absence of an effect of Rho kinases on H69 cell proliferation, the inactivation of Rho proteins by treatment of the cells with the clostridial fusion toxin C3-FT together with C2IIa (200 ng/mL each) did not affect cell proliferation (Fig. 4C).

To test whether the growth-inhibiting effects of $G\alpha_{12}$ and $G\alpha_{13}$ knockdown also occurred upon the stimulation of $G_{12/13}$ coupled receptors, we evaluated the proliferation of SCLC cells following treatment with bradykinin. Stimulation with bradykinin leads to the parallel activation of $G_{q/11}$ and $G_{12/13}$ signaling, and its mitogenic effects in SCLC cells are well established (21). Indeed, bradykinin treatment of H69 cells resulted in the stimulation of cell proliferation. However, this effect was largely reduced upon $G\alpha_{12}$ or $G\alpha_{13}$ targeting and was almost completely abolished upon $G\alpha_{12}/G\alpha_{13}$ double knockdown (Fig. 4D). These data strongly support the notion that $G\alpha_{12}$ and $G\alpha_{13}$ are involved in bradykinin-mediated stimulation of cell proliferation.

To ensure that $G_{q/11}$-dependent signaling was still functional upon $G\alpha_{12}$ or $G\alpha_{13}$ knockdown, we determined intracellular Ca^{2+} levels in H69 cells. These Ca^{2+} measurements revealed that downregulation of $G\alpha_{12}$

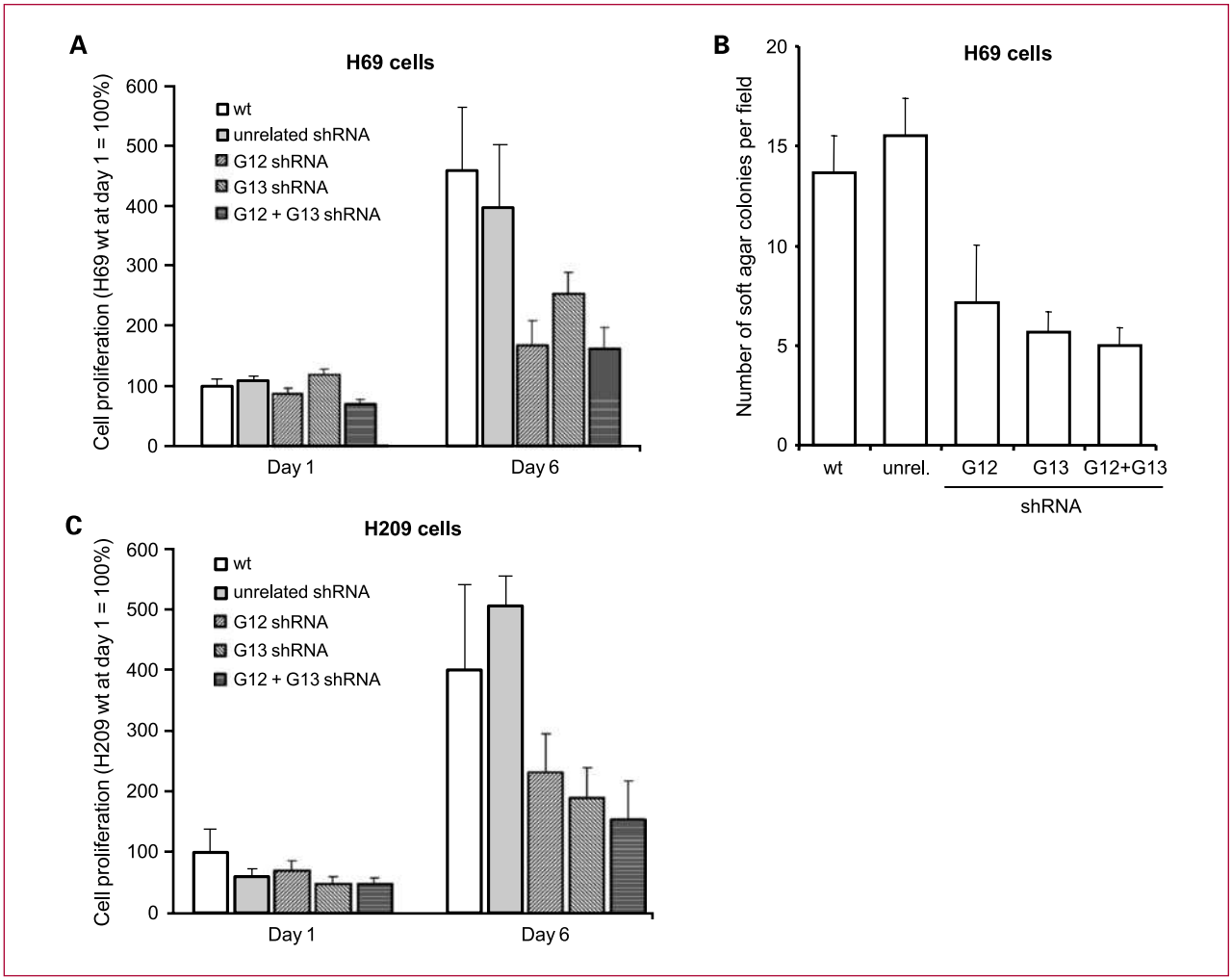

Fig. 3. Antiproliferative effects of shRNA-mediated downregulation of $G\alpha_{12}$ and $G\alpha_{13}$ in H69 and H209 SCLC cells. A, the compilation of several proliferation assays (day 1: time point of plating of the stable cell lines; day 6: cell densities 5 d after plating) establishes the reduced proliferation of H69 cells upon $G\alpha_{12}$ or $G\alpha_{13}$ targeting. No additive effects upon double targeting are observed. B, soft agar assay showing decreased colony formation of H69 cells upon shRNA-mediated $G\alpha_{12}$ or $G\alpha_{13}$ targeting. C, antiproliferative effects of shRNA-mediated downregulation of $G\alpha_{12}$ and $G\alpha_{13}$ in H209 SCLC cells. The compilation of several proliferation assays shows the reduced proliferation upon $G\alpha_{12}$ or $G\alpha_{13}$ targeting. No additive effects upon double targeting are observed.

Published OnlineFirst February 16, 2010; DOI: 10.1158/1078-0432.CCR-09-1873

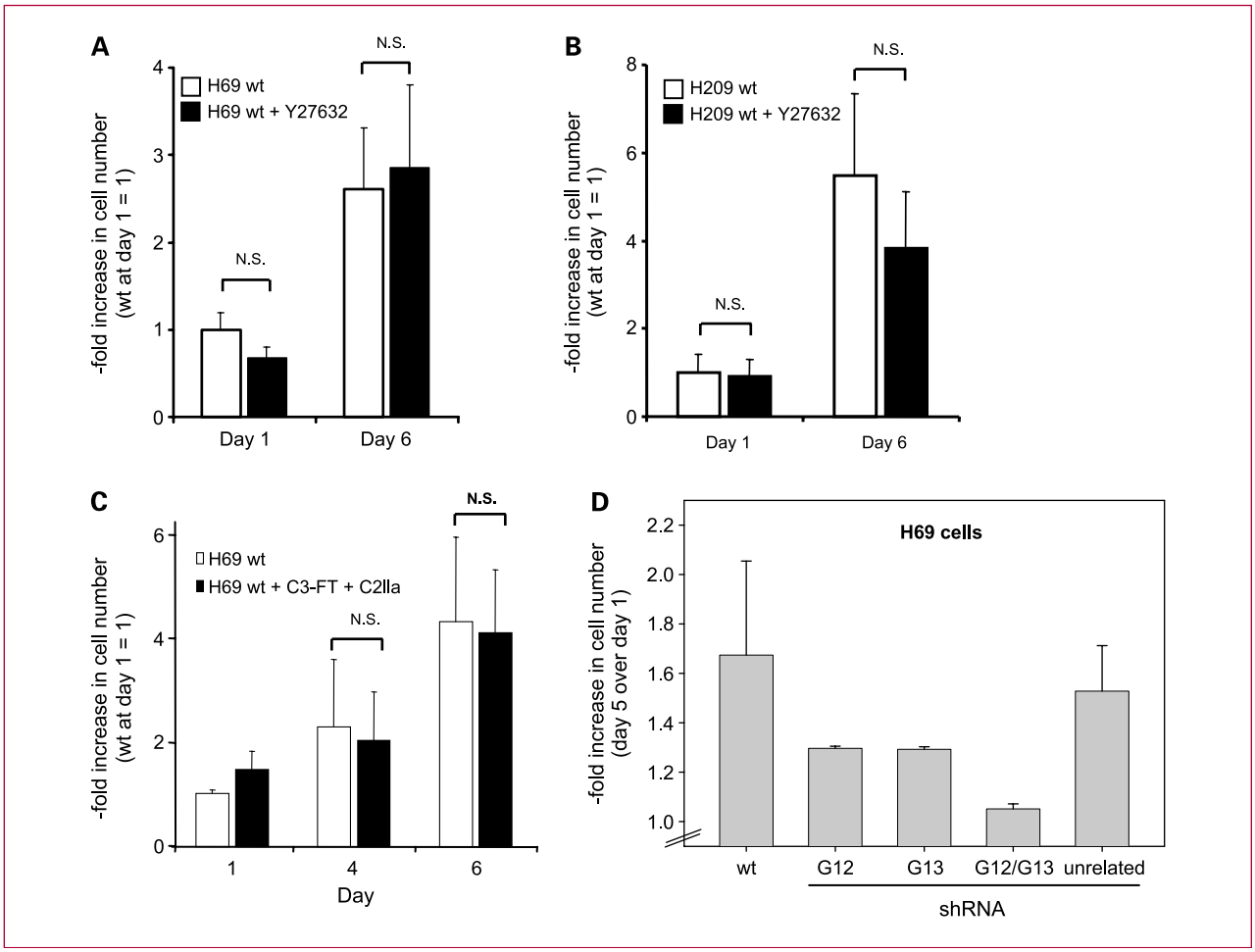

Fig. 4. H69 (A) and H209 (B) proliferation is independent of Rho/Rho kinase as shown by identical proliferation rates in the presence (black columns) or absence (white columns) of the Rho kinase inhibitor Y27632. C, likewise, no differences in proliferation are observed upon treatment (black columns) with a cell-permeable variant of clostridial C3 transferase, which inhibits Rho proteins, and with clostridial toxin B inhibiting Rho, Rac, and Cdc42. D, bradykinin-mediated stimulation of the proliferation of H69 cells grown in the presence of 10% FCS is inhibited upon $G\alpha_{12}$ or $G\alpha_{13}$ targeting. Double knockdown of both $G\alpha_{12}$ and $G\alpha_{13}$ leads to the almost complete abolishment of bradykinin stimulation.

and/or $G\alpha_{13}$ had no effect on basal intracellular Ca^{2+} levels (Supplementary Fig. S2). In addition, reduced $G\alpha_{12}$ and/or $G\alpha_{13}$ levels did not affect bradykinin-promoted increase in Ca^{2+} (Supplementary Fig. S3). Thus, the observed growth inhibition upon $G\alpha_{12}$ or $G\alpha_{13}$ knockdown is not mediated through alterations in Ca^{2+} signaling.

In vivo ***tumor growth of G_{12}/G_{13}-depleted SCLC cells.*** For the analysis of *in vivo* tumor growth, H69 cells virally infected with shRNAs as indicated in Fig. 5 were injected s.c. into athymic nude mice. While after an initial approximately 7- to 10-day lag phase, WT and control-infected cells rapidly formed nodules eventually resulting in large tumors, the growth of $G\alpha_{12}$ or $G\alpha_{13}$-depleted tumors was dramatically reduced by >50%. This decrease was statistically significant at day 19. After 4 weeks, the mean volume of the tumors infected with $G\alpha_{12}$- or $G\alpha_{13}$-specific shRNA amounted to only approximately 20% to 30% of control (Fig. 5). Antitumorigenic effects were also observed when investigating the initial tumor take, i.e., the total number of tumors formed after s.c. cell injection (Table 1). Although no differences were observed between WT, control, and $G\alpha_{13}$ shRNA-infected cells, tumorigenicity was markedly reduced upon $G\alpha_{12}$ targeting, thus suggesting different biological consequences of $G\alpha_{12}$ and $G\alpha_{13}$ depletion. Even more striking was the antitumorigenic effect upon the double targeting of $G\alpha_{12}$ and $G\alpha_{13}$, which completely abolished tumor growth, thus underscoring an additive role of both proteins in tumors *in vivo*. Comparable antitumor effects upon $G\alpha_{12}$ or $G\alpha_{13}$ single knockdown were obtained in H209 xenografts. Here, a generally poor tumor take was observed even in WT cells, which is in line with their poor colony formation properties in soft agar assays as mentioned above. This effect in combination with considerably larger variations in the initial tumor sizes prevented an analysis similarly accurate as in the

Published OnlineFirst February 16, 2010; DOI: 10.1158/1078-0432.CCR-09-1873

H69 xenografts. Still, when tumors, which were well established and within the same size range below 100 mm^3 after 4 weeks, were analyzed for their further growth rates, a ~25% decrease in tumor growth upon $G\alpha_{13}$ knockdown was observed. As seen in the previous *in vitro* experiments, $G\alpha_{12}$ knockdown resulted in more profound antitumor effects, which were also observed upon double knockdown (~65% reduction of tumor growth in both cell lines; data not shown).

For further analysis, the H69 xenografts were selected due to the larger number of tumor samples. Mice were sacrificed at day 28 and $G\alpha_{12}/G\alpha_{13}$ expression was determined on mRNA and protein levels. Quantitative RT-PCR revealed an ~40% reduction of $G\alpha_{12}$ or $G\alpha_{13}$ upon specific, shRNA-mediated targeting compared with the control groups (WT and unrelated shRNA infection), whereas the mRNA of the nontargeted protein ($G\alpha_{13}$ or $G\alpha_{12}$, respectively) remained unchanged (Fig. 6A and C). Because double targeting led to the complete abolishment of tumor growth, this group could not be included in the analysis. Concomitantly, the reduced mRNA levels translated into decreased $G\alpha_{12}/G\alpha_{13}$ protein levels as determined by immunohistochemistry. For quantification, paraffin sections were immunohistochemically stained for $G\alpha_{12}$ or $G\alpha_{13}$ and microscopically scanned under low magnification without hematoxilin counterstain (see Fig. 6B and D, right panel for representative areas). The subsequent determination of the brown staining intensities were done essentially as previously described (33) and revealed a robust (>70%) reduction of $G\alpha_{12}$ or $G\alpha_{13}$ protein levels, whereas expression in the control groups as well as levels of the nontargeted G protein remained unchanged (Fig. 6B and D, left). These results confirmed that the antitumorigenic effects were based on the specific downregulation of $G\alpha_{12}/G\alpha_{13}$. Finally, because our *in vitro* experiments indicated proliferative effects of $G\alpha_{12}/G\alpha_{13}$ expression in SCLC, tumor sections were stained for PCNA to determine the degree of proliferation in the different groups. Microscopic assessment of the percentage of proliferating cells revealed a slight but statistically significant decrease in cell proliferation by ~30% upon $G\alpha_{12}$ or $G\alpha_{13}$ targeting (Fig. 6E), indicating that observed differences in tumor growth are based on reduced tumor cell proliferation.

Differential activation of MAPK pathways. To assess the status of activation of various MAPK signal transduction pathways upon stable knockdown of $G\alpha_{12}$ or $G\alpha_{13}$, antibody arrays were done for H69 cells stably transfected with $G\alpha_{12}$ shRNA or with $G\alpha_{13}$ shRNA versus control shRNA, monitoring the phosphorylation of key signaling proteins. Signals showed considerable differences with regard to intensities, depending on the analyte. Therefore, the accurate detection of chemiluminescence relied on several different exposures (see Fig. 7 A and B, lower panel for representative examples) with signals close to the background or above the film saturation being excluded from quantitation.

For some signal transduction molecules, distinct differences between $G\alpha_{12}$ and $G\alpha_{13}$ knockdown were observed, supporting the notion that $G\alpha_{12}$ and $G\alpha_{13}$ may exert nonredundant functions in SCLC. For example, $G\alpha_{12}$ knockdown resulted in a profound reduction of HSP-27, RSK1, RSK2, and p38δ activation (Fig. 7A), whereas signals in $G\alpha_{13}$ cells (Fig. 7B) remained unchanged (RSK1, RSK2, and p38δ) or were strongly increased (HSP-27). The activation of other target proteins was only moderately changed upon $G\alpha_{12}$ or $G\alpha_{13}$ knockdown.

Most prominent, however, were the changes in ERK1/2 activation. Stable $G\alpha_{12}$ knockdown led to a marked activation of ERK1 (>2.5-fold) and ERK2 (>2-fold; Fig. 7A). Similar results were obtained in stably $G\alpha_{13}$ shRNA–expressing cells (Fig. 7B) indicating a tonic inhibition of the ERK pathway in SCLC by both $G\alpha_{12}$ and $G\alpha_{13}$. ERK1/2 activation was also seen in Western blots that

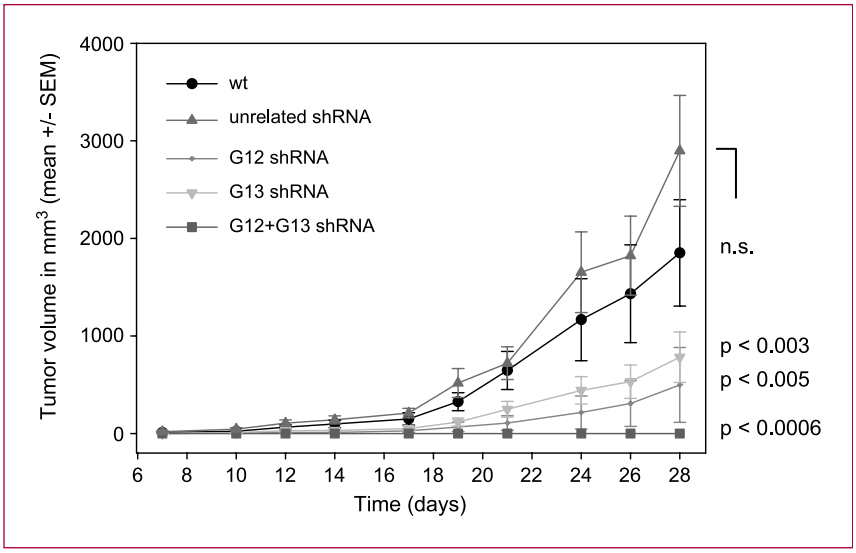

Fig. 5. shRNA-mediated double targeting of $G\alpha_{12}$ and $G\alpha_{13}$ abolishes tumor growth in a s.c. SCLC tumor xenograft mouse model. Single targeting of $G\alpha_{12}$ or $G\alpha_{13}$ results in reduced tumor growth compared with WT or control-infected H69 cells, with double targeting revealing an additive effect.

Published OnlineFirst February 16, 2010; DOI: 10.1158/1078-0432.CCR-09-1873

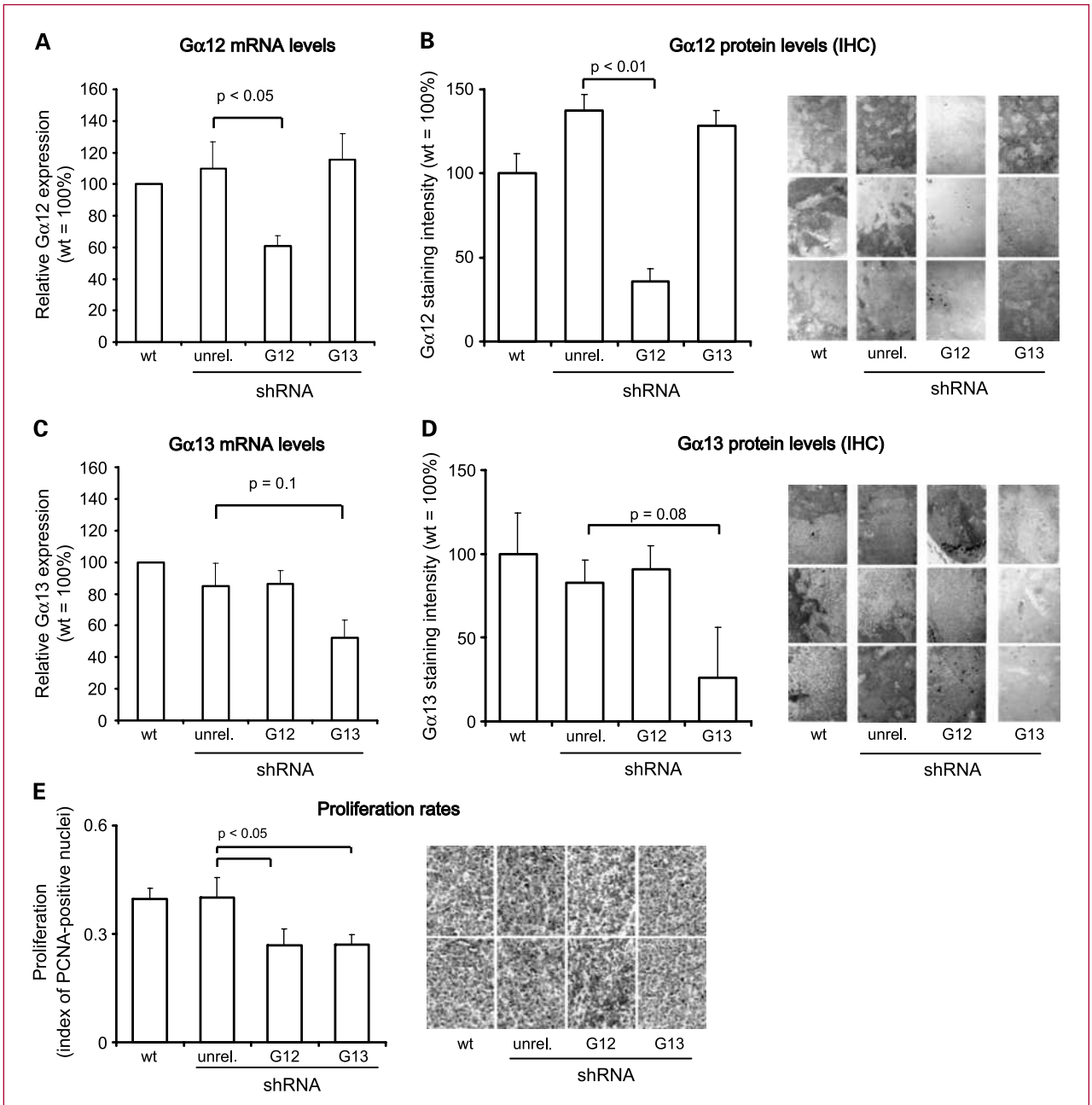

Fig. 6. Analysis of s.c. tumor xenografts form the SCLC mouse model. A to D, analysis of $G\alpha_{12}$ (A and B) and $G\alpha_{13}$ (C and D) expression on mRNA (A and C) and protein (B and D) levels in tumor xenografts derived from H69 cells stably transduced as indicated on the *X*-axis. B and D, right, fields representative for brown intensities (shown here in black and white) after immunohistochemical staining for $G\alpha_{12}$ (B) or $G\alpha_{13}$ (D), for better quantitation without hematoxylin counterstaining. E, reduced tumor cell proliferation upon $G\alpha_{12}$ or $G\alpha_{13}$ knockdown as shown by the immunohistochemical staining of the proliferation marker PCNA; left, quantitation of positive nuclei (brown); right, representative examples; positive nuclei appear as dark spots in this black and white reproduction.

showed a 1.5- to 2.7-fold increase of ERK2 phosphorylation upon stable knockdown of $G\alpha_{12}$ and/or $G\alpha_{13}$ (Fig. 7C), thus confirming the results from the antibody arrays. Because these data suggest that hyperactivity of ERK1/2 signaling could be responsible for the observed antiproliferative effects of $G\alpha_{12}$ or $G\alpha_{13}$ knockdown, it was also tested whether the inhibition of ERK1/2 could in turn induce proliferation. Indeed, the treatment of H69 cells with the ERK inhibitor U0126 led to increased proliferation (Fig. 7D).

Published OnlineFirst February 16, 2010; DOI: 10.1158/1078-0432.CCR-09-1873

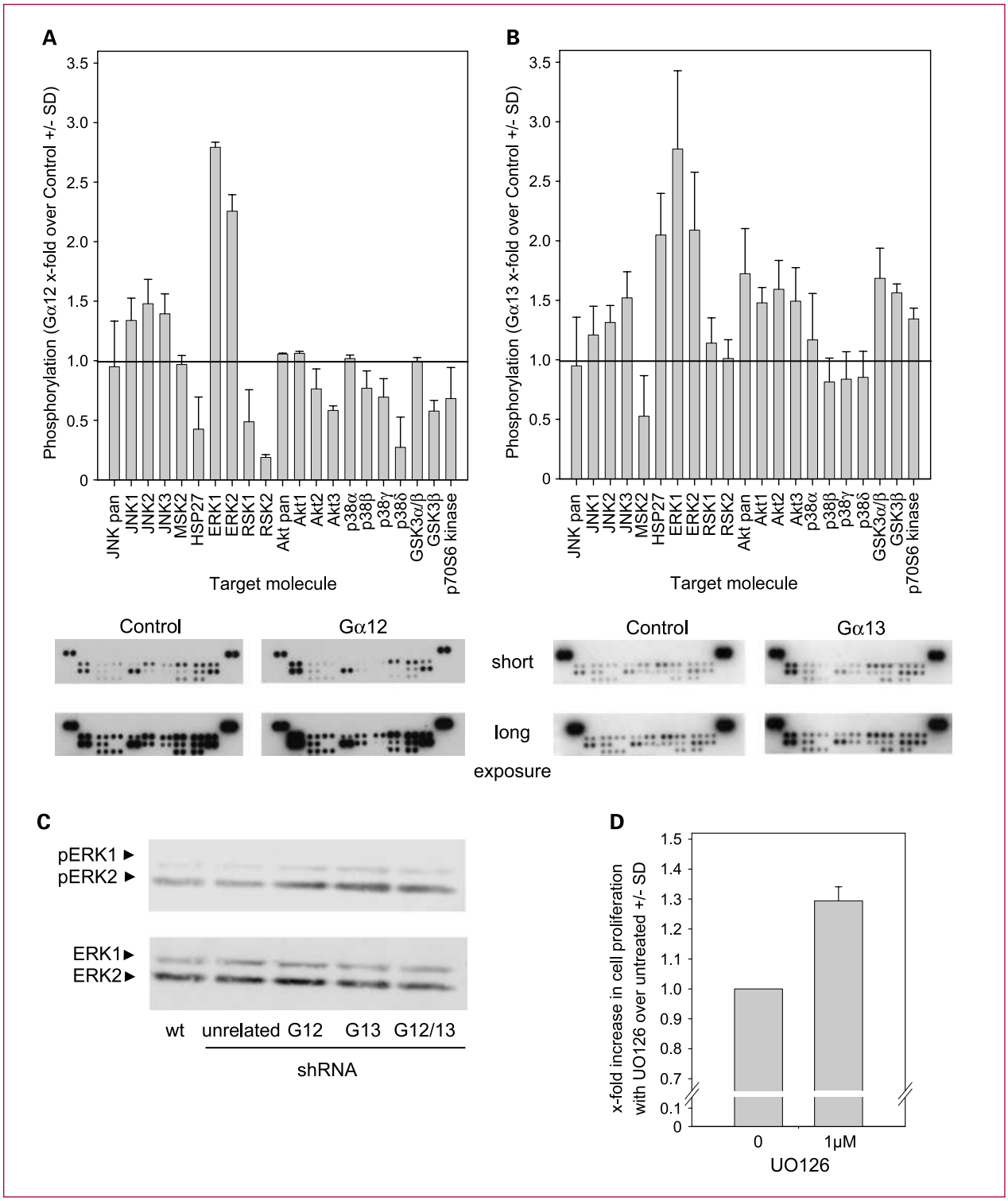

Fig. 7. Antibody arrays for the assessment of changes in the phosphorylation of various MAPK signal transduction pathways upon stable knockdown of $G\alpha_{12}$ or $G\alpha_{13}$. Arrays were probed with lysates from H69 cells stably transfected with control shRNA versus $G\alpha_{12}$ shRNA (A) or with control shRNA versus $G\alpha_{13}$ shRNA (B). Bottom, two representative examples of exposures per array used for quantitation (signals in the uppermost rows: loading controls; all other signals: analyte spots as dotted by the vendor, each in duplicates). Bar diagrams, differential activation of analyte molecules upon $G\alpha_{12}$ (A) or $G\alpha_{13}$ (B) knockdown, presented as x-fold over control. C, Western blots to confirm the increased ERK1/2 activation upon $G\alpha_{12}$ and/or $G\alpha_{13}$ knockdown. Increased levels of pERK1 and pERK2 are observed in stable $G\alpha_{12}$, $G\alpha_{13}$, and double knockdown cells. D, increased proliferation of H69 cells upon treatment with the ERK inhibitor U0126.

Published OnlineFirst February 16, 2010; DOI: 10.1158/1078-0432.CCR-09-1873

Discussion

The dependence of SCLC on mitogenic signaling of G proteins has been well established, and a mitogenic function of $G_{12/13}$ signaling has been discussed because the expression of WT $G\alpha_{12}$ is sufficient to confer malignant growth characteristics on fibroblasts (6, 7). However, the contributions of $G\alpha_{12}$ and of $G\alpha_{13}$ to the malignant phenotype of SCLC still remain elusive. Furthermore, the transforming activities of $G\alpha_{12}$ and $G\alpha_{13}$ were shown to be not redundant because overexpression of $G\alpha_{13}$ does not exhibit effects in fibroblasts comparable with $G\alpha_{12}$ (34). This requires a separate assessment of $G\alpha_{12}$ and $G\alpha_{13}$ functions in SCLC. In breast and prostate cancer cells, previous studies showed a role of $G\alpha_{12}$ and of $G\alpha_{13}$ in invasiveness, but not in tumor cell proliferation (9, 10).

In contrast, we show in this article that in SCLC cells, the downregulation of either $G\alpha_{12}$ or $G\alpha_{13}$ leads to a clear inhibition of proliferation *in vitro* as well as *in vivo*. Strikingly, the *in vivo* data also reveal an additive effect of $G\alpha_{12}$ and $G\alpha_{13}$ depletion, with double targeting of both proteins leading to complete abolishment of tumor growth. This seminal finding further supports the concept that intact $G_{12/13}$ signaling is a prerequisite for tumor growth in SCLC.

Expression of shRNA against $G\alpha_{12}$ or $G\alpha_{13}$ by a lentiviral system elicited a sustained and efficient downregulation of the respective target in SCLC cells, an effect still detectable after 2 months *in vitro* culture or after >1 month *in vivo* growth in xenografted nude mice. This long-term stability reflects the genomic integration of lentivirally delivered shRNA-coding constructs, thus allowing the loss-of-function analyses done here. The stable downregulation used here, as opposed to transient targeting or stimulation approaches, also mimicks a prolonged therapeutic intervention. Furthermore, the use of shRNA-mediated gene targeting rather than inhibitors allowed to precisely distinguish between G_{12} and G_{13} signaling regarding the biological function. Notably, the persistent downregulation of $G\alpha_{12}$ did not lead to a compensatory upregulation of $G\alpha_{13}$ and vice versa. Likewise, no changes in $G\alpha_{11}$ or $G\alpha_{q}$ expression were observed. The latter observation as well as the correlation between knockdown efficacies and antiproliferative effects of the various shRNA constructs also suggests the absence of off-target effects, although the possibility of nonspecific effects can never be completely excluded.

Regarding G protein–dependent signaling and its effects on proliferation of SCLC cells, the best characterized pathway emanates from the activation of $G_{q/11}$ (e.g., through stimulation with neuropeptides), which leads to the activation of the phospholipase Cβ-PKC cascade and to a increase in intracellular calcium ($[Ca^{2+}]_i$; ref. 21). Elevated $[Ca^{2+}]_i$ stimulates ERK1/2 through the activation of Pyk2 and Src kinases, and subsequently Ras (35). In contrast, our knowledge on biological functions and molecular effectors of $G_{12/13}$ signaling (11) in SCLC cells is rather limited. Neuropeptide-promoted stimulation of $G_{12/13}$ has been shown to lead to the activation of monomeric GTPases of the Rho family (20, 36), and a pivotal role of Rho proteins as effectors of $G_{12/13}$ signaling in SCLC cells is suggested by the fact that Rho proteins show particularly high expression levels in these tumors (23, 37). Rho and Rho kinase are involved in transendothelial migration of SCLC cells (38). Furthermore, a $G_{12/13}$ and Rho-dependent signaling pathway has been described involving the activation of Pyk2, which could represent a point of convergence for $G_{q/11}$ (see above) and $G_{12/13}$-dependent signaling (39). However, the inactivation of Rho proteins through clostridial C3 exoenzyme did not alter the proliferation of SCLC cells in our study, whereas proliferation of NSCLC cells was decreased (22, 23). This agrees with our findings that the pharmacologic inhibition of Rho kinase, a downstream effector of Rho proteins, did not inhibit the growth of H69 and H209 cells. Thus, we conclude that the activation of the Rho-Rho kinase pathway does not seem to represent a critical component of the $G_{12/13}$-dependent proliferation pathways.

On the other hand, numerous $G_{12/13}$-dependent and Rho-independent potential mitogenic pathways have been suggested, which are mediated, e.g., through Rac (40, 41), ERK5 (42), and the cadherin-catenin complex (43, 44). Thus, other molecular effectors are potential candidates to contribute to the $G_{12/13}$-dependent mitogenic signaling in SCLC cells. In fact, our data obtained from the antibody array indicate that additional pathways that have not been implicated in $G_{12/13}$ signaling thus far seem to be involved. Conversely, certain signal transduction modules previously described as downstream effectors of $G_{12/13}$ do not seem to play a major role in SCLC. For example, it was shown in SCLC cells that $G_{12/13}$ stimulation through UV radiation or treatment of cells with $G_{12/13}$-stimulating biased agonists inhibits proliferation through the activation of c-Jun-NH_2-kinase (24, 45). This conclusion is not supported by our experiments at least for the SCLC cell line used here because in the antibody array, only minor changes, if any at all, are observed upon stable $G\alpha_{12}$ or $G\alpha_{13}$ knockdown. However, it should also be noted that previous studies relied on short-term agonist treatment, whereas in our experiments, stable cell lines were analyzed. Thus, potential adaptive processes upon prolonged inhibition of $G_{12/13}$ signaling have to be taken into account (see below).

$G\alpha_{12}$, but not $G\alpha_{13}$, knockdown led to a marked >50% inactivation of Hsp27. Heat shock proteins including Hsp27, which are induced in cells exposed to stress and which function as molecular chaperons involved in protein folding, have been implicated in cancer (46), and Hsp27 is expressed in the majority of non-SCLC (47). Because Hsp27 is involved in cell growth, the reduction of activated Hsp27 upon G_{12} knockdown may add to the antiproliferative effects observed in our study. In contrast, stable targeting of $G\alpha_{13}$ even results in the enhanced phosphorylation levels of Hsp27. This observation underlines

Published OnlineFirst February 16, 2010; DOI: 10.1158/1078-0432.CCR-09-1873

that G_{12} and G_{13} signaling targets different downstream effectors and further strengthens the concept of nonredundant functions of G_{12} and G_{13} pathways.

The most pronounced effect in response to $G\alpha_{12}$ or $G\alpha_{13}$ knockdown was an increased ERK1/2 activation as detected by the antibody array and subsequently confirmed by Western blotting with phosphoERK1/2-specific antibodies. ERK1/2 activity usually correlates positively with cell proliferation—a notion that seems to contradict the cellular phenotype observed in our stably $G_{12/13}$-downregulated cell lines. However, the finding of growth suppression upon hyperactivity of ERK1/2 was supported by our ERK inhibitor experiments, and a more complex function of ERK1/2 has emerged by detailed studies in different cell models. In fact, in the case of SCLC, it has been shown that overstimulation of the Ras-MAP/ERK kinase-ERK cascade following the expression of constitutively active Ras or the overexpression of Raf-1 leads to growth arrest and apoptosis (13, 48–50). Thus, the elevated basal phosphorylation of ERK1/2 upon $G\alpha_{12}$ or $G\alpha_{13}$ knockdown may indicate an analogously disbalanced signaling. One possibility in this context would be that the inhibition of $G_{12/13}$ signaling leads to the increased activation of $G_{q/11}$-dependent pathways. $G_{q/11}$-promoted signaling has been shown to stimulate the Ca^{2+}-dependent tyrosine kinase Pyk2 and to subsequently cause the activation of the Ras-ERK cascade (35). In a balanced signaling context, this pathway exerts mitogenic effects in SCLC cells (35). In contrast, overexpression of Pyk2 in SCLC cells leads to growth arrest and apoptosis,[3] suggesting that the uncontrolled activation of this pathway is antiproliferative in SCLC cells. However, $G\alpha_{12}$ or $G\alpha_{13}$ knockdown affected neither basal Ca^{2+} levels (Supplementary Fig. S2) nor the bradykinin-stimulated increase in Ca^{2+} concentration (Supplementary Fig. S3). This suggests that the downregulation of $G\alpha_{12}$ or $G\alpha_{13}$ does not interfere with $G_{q/11}$-mediated signaling.

Depending on the cell type, ERK1/2 activation has been shown to occur through different pathways that distinctly define the duration and cellular distribution of activated ERK1/2. More specifically, RSK activation seems to be achieved only by transient rather than sustained activation of ERK1/2 (51). As the antibody array data obtained from unstimulated cells reflects constitutive activation or inactivation of signaling proteins, the parallel increased phosphorylation status of ERK1/2 and the concomitant dephosphorylation and inactivation of RSK in $G\alpha_{12}$-depleted cells conforms to the latter concept.

Taken together, our data show that $G\alpha_{12}$ and $G\alpha_{13}$ knockdown results in multifacetted cellular responses that will require further analysis. The selective knockdown of $G\alpha_{12}$ and $G\alpha_{13}$ in SCLC cells presented herein proves that both proteins, $G\alpha_{12}$ and $G\alpha_{13}$, exert nonredundant proliferative effects in SCLC cells. It represents a promising approach to identify the downstream targets of these G proteins critically involved in the proliferation in SCLC cells and may help in further dissecting the nonredundant functions of $G\alpha_{12}$ and $G\alpha_{13}$ in these tumors. The complete abolishment of tumor growth upon parallel shRNA-mediated targeting of $G\alpha_{12}$ and $G\alpha_{13}$ also shows the increased therapeutic efficacy of RNAi-based double knockdown approaches of nonredundant, but closely related tumor-relevant gene products.

[3] T. Büch, T. Gudermann, A. Aigner, unpublished data.

Disclosure of Potential Conflicts of Interest

No potential conflicts of interest were disclosed.

Acknowledgments

We thank Johanna Platzek, Damian Stebel, and Andrea Wüstenhagen for the expert help with the experiments; Fatma Aktuna for preparing the tissue sections; and Didier Trono for providing pLVTHM, pMD2G, and psPAX2 plasmids.

Grant Support

Deutsche Forschungsgemeinschaft SFB-Transregio 17 (T. Gudermann and A. Aigner) and Deutsche Forschungsgemeinschaft-Forschergruppe 627 (A. Aigner).

The costs of publication of this article were defrayed in part by the payment of page charges. This article must therefore be hereby marked *advertisement* in accordance with 18 U.S.C. Section 1734 solely to indicate this fact.

Received 07/16/2009; revised 12/22/2009; accepted 12/23/2009; published OnlineFirst 02/16/2010.

References

1. Daaka Y. G proteins in cancer: the prostate cancer paradigm. Sci STKE 2004;2004:re2.
2. Fields TA, Casey PJ. Signalling functions and biochemical properties of pertussis toxin-resistant G-proteins. Biochem J 1997;321:561–71.
3. Pierce KL, Premont RT, Lefkowitz RJ. Seven-transmembrane receptors. Nat Rev Mol Cell Biol 2002;3:639–50.
4. Dorsam RT, Gutkind JS. G-protein-coupled receptors and cancer. Nat Rev Cancer 2007;7:79–94.
5. Radhika V, Dhanasekaran N. Transforming G proteins. Oncogene 2001;20:1607–14.
6. Chan AM, Fleming TP, McGovern ES, Chedid M, Miki T, Aaronson SA. Expression cDNA cloning of a transforming gene encoding the wild-type G α 12 gene product. Mol Cell Biol 1993;13:762–8.
7. Xu N, Bradley L, Ambdukar I, Gutkind JS. A mutant α subunit of G12 potentiates the eicosanoid pathway and is highly oncogenic in NIH 3T3 cells. Proc Natl Acad Sci U S A 1993;90:6741–5.
8. Juneja J, Casey PJ. Role of G12 proteins in oncogenesis and metastasis. Br J Pharmacol 2009;158:32–40.
9. Kelly P, Moeller BJ, Juneja J, et al. The G12 family of heterotrimeric G proteins promotes breast cancer invasion and metastasis. Proc Natl Acad Sci U S A 2006;103:8173–8.
10. Kelly P, Stemmle LN, Madden JF, Fields TA, Daaka Y, Casey PJ. A

Published OnlineFirst February 16, 2010; DOI: 10.1158/1078-0432.CCR-09-1873

role for the G12 family of heterotrimeric G proteins in prostate cancer invasion. J Biol Chem 2006;281:26483–90.
11. Kelly P, Casey PJ, Meigs TE. Biologic functions of the G12 subfamily of heterotrimeric g proteins: growth, migration, and metastasis. Biochemistry 2007;46:6677–87.
12. Govindan R, Page N, Morgensztern D, et al. Changing epidemiology of small-cell lung cancer in the United States over the last 30 years: analysis of the surveillance, epidemiologic, and end results database. J Clin Oncol 2006;24:4539–44.
13. Rozengurt E. Autocrine loops, signal transduction, and cell cycle abnormalities in the molecular biology of lung cancer. Curr Opin Oncol 1999;11:116–22.
14. Zochbauer-Muller S, Gazdar AF, Minna JD. Molecular pathogenesis of lung cancer. Ann Rev Physiol 2002;64:681–708.
15. Song P, Sekhon HS, Lu A, et al. M3 muscarinic receptor antagonists inhibit small cell lung carcinoma growth and mitogen-activated protein kinase phosphorylation induced by acetylcholine secretion. Cancer Res 2007;67:3936–44.
16. Seckl MJ, Higgins T, Widmer F, Rozengurt E. [D-Arg1,D-Trp5,7,9, Leu11]substance P: a novel potent inhibitor of signal transduction and growth *in vitro* and *in vivo* in small cell lung cancer cells. Cancer Res 1997;57:51–4.
17. Langdon S, Sethi T, Ritchie A, Muir M, Smyth J, Rozengurt E. Broad spectrum neuropeptide antagonists inhibit the growth of small cell lung cancer *in vivo*. Cancer Res 1992;52:4554–7.
18. Everard MJ, Macaulay VM, Miller JL, Smith IE. *In vitro* effects of substance P analogue [D-Arg1, D-Phe5, D-Trp7,9, Leu11] substance P on human tumour and normal cell growth. Br J Cancer 1992;65:388–92.
19. Woll PJ, Rozengurt E. A neuropeptide antagonist that inhibits the growth of small cell lung cancer *in vitro*. Cancer Res 1990;50:3968–73.
20. Wittau N, Grosse R, Kalkbrenner F, Gohla A, Schultz G, Gudermann T. The galanin receptor type 2 initiates multiple signaling pathways in small cell lung cancer cells by coupling to G(q), G(i) and G(12) proteins. Oncogene 2000;19:4199–209.
21. Gudermann T, Roelle S. Calcium-dependent growth regulation of small cell lung cancer cells by neuropeptides. Endocr Related Cancer 2006;13:1069–84.
22. Tokman MG, Porter RA, Williams CL. Regulation of cadherin-mediated adhesion by the small GTP-binding protein Rho in small cell lung carcinoma cells. Cancer Res 1997;57:1785–93.
23. Varker KA, Phelps SH, King MM, Williams CL. The small GTPase RhoA has greater expression in small cell lung carcinoma than in non-small cell lung carcinoma and contributes to their unique morphologies. IntJ Oncol 2003;22:671–81.
24. Chan D, Gera L, Stewart J, et al. Bradykinin antagonist dimer, CU201, inhibits the growth of human lung cancer cell lines by a "biased agonist" mechanism. Proc Natl Acad Sci U S A 2002;99:4608–13.
25. Gu JL, Muller S, Mancino V, Offermanns S, Simon MI. Interaction of G α (12) with G α (13) and G α (q) signaling pathways. Proc Natl Acad Sci U S A 2002;99:9352–7.
26. Reynolds A, Leake D, Boese Q, Scaringe S, Marshall WS, Khvorova A. Rational siRNA design for RNA interference. Nat Biotechnol 2004;22:326–30.
27. Elbashir SM, Harborth J, Weber K, Tuschl T. Analysis of gene function in somatic mammalian cells using small interfering RNAs. Methods 2002;26:199–213.
28. Hahn A, Barth H, Kress M, Mertens PR, Goppelt-Struebe M. Role of Rac and Cdc42 in lysophosphatidic acid-mediated cyclo-oxygenase-2 gene expression. Biochem J 2002;362:33–40.
29. Wellstein A, Lupu R, Zugmaier G, et al. Autocrine growth stimulation by secreted Kaposi's fibroblast growth factor but not by endogenous basic fibroblast growth factor. Cell Growth Differ 1990;1:63–71.
30. Aigner A, Ray PE, Czubayko F, Wellstein A. Immunolocalization of an FGF-binding protein reveals a widespread expression pattern during different stages of mouse embryo development. Histochem Cell Biol 2002;117:1–11.
31. Werth S, Urban-Klein B, Dai L, et al. A low molecular weight fraction of polyethylenimine (PEI) displays increased transfection efficiency of DNA and siRNA in fresh or lyophilized complexes. J Control Release 2006;112:257–70.
32. Ito M, Nakano T, Erdodi F, Hartshorne DJ. Myosin phosphatase: structure, regulation and function. Mol Cell Biochem 2004;259:197–209.
33. Urban-Klein B, Werth S, Abuharbeid S, Czubayko F, Aigner A. RNAi-mediated gene-targeting through systemic application of polyethylenimine (PEI)-complexed siRNA *in vivo*. Gene Ther 2005;12:461–6.
34. Radhika V, Hee Ha J, Jayaraman M, Tsim ST, Dhanasekaran N. Mitogenic signaling by lysophosphatidic acid (LPA) involves Gα12. Oncogene 2005;24:4597–603.
35. Roelle S, Grosse R, Buech T, Chubanov V, Gudermann T. Essential role of Pyk2 and Src kinase activation in neuropeptide-induced proliferation of small cell lung cancer cells. Oncogene 2008;27:1737–48.
36. Beekman A, Helfrich B, Bunn PA, Jr., Heasley LE. Expression of catalytically inactive phospholipase Cβ disrupts phospholipase Cβ and mitogen-activated protein kinase signaling and inhibits small cell lung cancer growth. Cancer Res 1998;58:910–3.
37. Touge H, Chikumi H, Igishi T, et al. Diverse activation states of RhoA in human lung cancer cells: contribution of G protein coupled receptors. IntJ Oncol 2007;30:709–15.
38. Li B, Zhao WD, Tan ZM, Fang WG, Zhu L, Chen YH. Involvement of Rho/ROCK signalling in small cell lung cancer migration through human brain microvascular endothelial cells. FEBS Lett 2006;580:4252–60.
39. Shi CS, Sinnarajah S, Cho H, Kozasa T, Kehrl JH. G13α-mediated PYK2 activation. PYK2 is a mediator of G13α -induced serum response element-dependent transcription. J Biol Chem 2000;275:24470–6.
40. Liu G, Voyno-Yasenetskaya TA. Radixin stimulates Rac1 and Ca2+/calmodulin-dependent kinase, CaMKII: cross-talk with Gα13 signaling. J Biol Chem 2005;280:39042–9.
41. Vaiskunaite R, Adarichev V, Furthmayr H, Kozasa T, Gudkov A, Voyno-Yasenetskaya TA. Conformational activation of radixin by G13 protein α subunit. J Biol Chem 2000;275:26206–12.
42. Fukuhara S, Marinissen MJ, Chiariello M, Gutkind JS. Signaling from G protein-coupled receptors to ERK5/Big MAPK 1 involves Gα q and Gα 12/13 families of heterotrimeric G proteins. Evidence for the existence of a novel Ras AND Rho-independent pathway. J Biol Chem 2000;275:21730–6.
43. Meigs TE, Fedor-Chaiken M, Kaplan DD, Brackenbury R, Casey PJ. Gα12 and Gα13 negatively regulate the adhesive functions of cadherin. J Biol Chem 2002;277:24594–600.
44. Meigs TE, Fields TA, McKee DD, Casey PJ. Interaction of Gα 12 and Gα 13 with the cytoplasmic domain of cadherin provides a mechanism for β -catenin release. Proc Natl Acad Sci U S A 2001;98:519–24.
45. Butterfield L, Storey B, Maas L, Heasley LE. c-Jun NH2-terminal kinase regulation of the apoptotic response of small cell lung cancer cells to ultraviolet radiation. J Biol Chem 1997;272:10110–6.
46. Sarto C, Binz PA, Mocarelli P. Heat shock proteins in human cancer. Electrophoresis 2000;21:1218–26.
47. Huang Q, Zu Y, Fu X, Wu T. Expression of heat shock protein 70 and 27 in non-small cell lung cancer and its clinical significance. J Huazhong Univ Sci Technolog Med Sci 2005;25:693–5.
48. Mabry M, Nakagawa T, Nelkin BD, et al. v-Ha-ras oncogene insertion: a model for tumor progression of human small cell lung cancer. Proc Natl Acad Sci U S A 1988;85:6523–7.
49. Mabry M, Nakagawa T, Baylin S, Pettengill O, Sorenson G, Nelkin B. Insertion of the v-Ha-ras oncogene induces differentiation of calcitonin-producing human small cell lung cancer. J Clin Invest 1989;84:194–9.
50. Ravi RK, Weber E, McMahon M, et al. Activated Raf-1 causes growth arrest in human small cell lung cancer cells. J Clin Invest 1998;101:153–9.
51. Shah BH, Farshori MP, Jambusaria A, Catt KJ. Roles of Src and epidermal growth factor receptor transactivation in transient and sustained ERK1/2 responses to gonadotropin-releasing hormone receptor activation. J Biol Chem 2003;278:19118–26.

Published OnlineFirst February 16, 2010; DOI: 10.1158/1078-0432.CCR-09-1873

Clinical Cancer Research

Critical Role of $G\alpha_{12}$ and $G\alpha_{13}$ for Human Small Cell Lung Cancer Cell Proliferation *In vitro* and Tumor Growth *In vivo*

Marius Grzelinski, Olaf Pinkenburg, Thomas Büch, et al.

Clin Cancer Res 2010;16:1402-1415. Published OnlineFirst February 16, 2010.